Journal of Applied Sciences and Applications in Engineering

SCIVOLVE

Research Article

Open Access Full Text Article

# Comparative Synthesis, Spectroscopic Characterization and Concentration-Dependent Antimicrobial Profiling of 8-Substituted 2,5-Dihydro-1,5-Benzothiazepines

**N. P. Singh[*1], Anita Rai[2], Sanjay Kumar Singh[3]**

[1*]Associate Professor, Department of Chemistry, DBS PG College, Govind Nagar, Kanpur, India.
[2]Department of Chemistry, PPN PG College, Kanpur, India.
[3]Associate Professor, Department of Chemistry, DBS PG College, Govind Nagar, Kanpur, India.

**Correspondence:**
N. P. Singh, Associate Professor, Department of Chemistry, DBS PG College, Govind Nagar, Kanpur, India.

**Received:** September 03, 2026; **Published:** September 17, 2026

**How to cite this article:**
Singh, N. P., Rai, A., Singh, S. K. (2026). Comparative Synthesis, Spectroscopic Characterization and Concentration-Dependent Antimicrobial Profiling of 8-Substituted 2,5-Dihydro-1,5-Benzothiazepines. *Journal of Applied Sciences and Applications in Engineering, 2*(2), 1–8. doi: 10.64978/jasae.2026.09170105

## Abstract

A matched library of twelve 8-substituted 2,5-dihydro-1,5-benzothiazepines was synthesized by trifluoroacetic-acid-catalyzed cyclocondensation of six 5-substituted 2-aminobenzenethiols with either a naphthyl chalcone (series A, 5a–5f) or a 2,4-dichlorophenyl chalcone (series B, 5g–5l). Isolated yields were 60–70%. Structures were supported by elemental analysis, IR, $^1$H NMR and, for representative halo derivatives, isotope-pattern mass spectrometry. Antimicrobial activity was measured by agar-well diffusion against Escherichia coli, Pseudomonas aeruginosa, Staphylococcus aureus and Candida albicans at 25, 50, 75 and 100 µg mL$^{-1}$. We performed a fresh descriptive analysis of 188 reported compound–organism–concentration observations, retaining four entries reported as not available as missing rather than converting them to zero. Activity indices were recomputed against the concentration-matched reference drugs. Compound 5j had the highest mean activity index across available cells, although one missing cell makes that ranking sensitive to missingness; among complete profiles, 5a ranked highest. At 100 µg mL$^{-1}$, 5c gave the largest mean inhibition zone (15.5 mm) and the strongest response against S. aureus (19 mm). All compounds displayed broadly concentration-dependent inhibition, but none matched the reference drugs across the complete panel. Matched-pair comparisons indicated that changing the aryl scaffold from naphthyl to 2,4-dichlorophenyl did not produce a uniform activity gain; the direction depended on the 8-substituent and organism. Because the thesis dataset contains single reported zone values without replicate-level dispersion, all rankings and correlations are exploratory. The results prioritize 5c, 5a, 5f and 5h for confirmatory broth microdilution, replicate testing and cytotoxicity evaluation.

**Keywords:** 1,5-benzothiazepine; chalcone; cyclocondensation; agar-well diffusion; antimicrobial activity; activity index; structure–activity relationship; descriptive reanalysis.

### Highlights

- Twelve matched 8-substituted analogues were obtained in 60–70% isolated yield.
- All 188 available antimicrobial measurements were reanalyzed without imputing missing values.
- Compound 5c led the high-dose ranking and reached 19 mm against S. aureus at 100 µg mL$^{-1}$.
- Scaffold replacement produced substituent-dependent, not uniform, activity changes.

## Introduction

Antimicrobial resistance continues to erode the effectiveness of established therapies. The World Health Organization's 2025 global surveillance report synthesizes more than 23 million bacteriologically confirmed infections and highlights the breadth and persistence of resistance across major pathogens (World Health Organization [WHO], 2025). This pressure strengthens the case for chemically diverse screening libraries, but it also raises the evidentiary standard: preliminary inhibition-zone data should

be interpreted as lead-generation evidence rather than as clinical susceptibility endpoints (Clinical and Laboratory Standards Institute [CLSI], 2024; Clinical and Laboratory Standards Institute [CLSI], 2026).

Seven-membered nitrogen–sulfur heterocycles occupy a distinctive region of medicinal-chemistry space. The 1,5-benzothiazepine scaffold combines conformational flexibility with two heteroatoms that can influence electronics, hydrogen bonding and lipophilicity. Its pharmacological visibility is reinforced by clinically used benzothiazepine-related agents and by reported antimicrobial, anticancer, antidiabetic and central nervous system activities (Bariwal et al., 2008; Bhabal et al., 2022; Dhiaa et al., 2023; Haroun et al., 2022; Ogunnupebi et al., 2023; Saha et al., 2015; Shaik et al., 2020; Suman et al., 2024). Recent reviews emphasize continued innovation in annulation, green synthesis and fused or hybrid benzothiazepine design (Chaudhri, 2022; Devi et al., 2020; Gharge & Alegaon, 2024; Kosmalski et al., 2024; Pathania et al., 2019; Qadir et al., 2022; Ronse et al., 2023; Suman et al., 2023).

Cyclocondensation of o-aminothiophenols with α, β-unsaturated carbonyl compounds remains a direct entry to 2,3- or 2,5-dihydro-1,5-benzothiazepines (Suman et al., 2023; Chate et al., 2011; Mange et al., 2007). Chalcones are especially useful precursors because their two aryl regions provide controlled variation while preserving a shared reaction manifold. In biological studies, however, comparisons are often complicated by changes in scaffold, substituent, assay concentration and reference drug. A matched series, analyzed on a common normalized scale, can reveal whether a scaffold exchange behaves consistently or interacts with the peripheral substituent.

The underlying thesis generated two matched six-member series that differ primarily in one aryl domain: a naphthyl group in series A and a 2,4-dichlorophenyl group in series B. Each series contains methoxy, methyl, ethoxy, fluoro, chloro and bromo substitution at the 8-position. The complete set was evaluated against two Gram-negative bacteria, one Gram-positive bacterium and one yeast over four concentrations. This structure makes the dataset suitable for a fresh, transparent reanalysis.

The present paper therefore had four objectives: (i) consolidate the synthesis and spectroscopic evidence for the twelve compounds; (ii) recompute concentration-specific activity indices directly from the reported zones and reference-drug values; (iii) compare compound ranking, organism selectivity and matched scaffold effects; and (iv) identify defensible leads and the experimental work needed before potency claims can be strengthened. No unreported measurements were generated or imputed.

## Materials and methods

### Study design and data provenance

This original research article is based on the experimental synthesis, characterization and antimicrobial measurements reported in Chapter III of the authors' thesis materials. Numerical values were transcribed into a tidy analysis table in which each row represents one compound–organism–concentration combination. The two chemical series were preserved exactly as reported. Four cells marked 'NA' in the source were encoded as missing. They were not interpreted as absence of activity because the reason for non-reporting was not documented.

### General chemistry

Melting points were recorded in open capillaries and are uncorrected. Reaction progress and product purity were monitored by thin-layer chromatography using benzene/ethanol/50% aqueous ammonia (7:2:1, v/v/v). IR spectra were recorded as KBr pellets on a PerkinElmer Spectrum instrument. $^1$H NMR spectra were acquired at 400 MHz with tetramethylsilane as internal reference; the source tables identify DMSO-$d_6$ for series A and $CDCl_3$ for series B. DART mass spectra were acquired using a JEOL AccuTOF JMS-T100LC instrument. Elemental analyses were carried out at the Materials Research Centre, MNIT Jaipur.

### Chalcone synthesis

The required chalcones were prepared by base-catalyzed Claisen–Schmidt condensation. Equimolar 2-acetylnaphthalene or 2,4-dichloroacetophenone and 4-methoxybenzaldehyde were combined in dry ethanol, treated with 40% KOH and allowed to react under the conditions described in the thesis. Acidification afforded crystalline chalcones 3a and 3b in 73.0% and 68.22% yield, respectively. Their melting points (98 °C and 121 °C) were consistent with the reported values cited in the thesis.

### General synthesis of compounds 5a–5l

A chalcone (0.001 mol) and the appropriate 5-substituted 2-aminobenzenethiol (0.001 mol) were dissolved in dry ethanol (15 mL). Trifluoroacetic acid was added as catalyst and the mixture was refluxed, typically for 3–5 h, with TLC monitoring. After cooling, the products were isolated and recrystallized from dry ethanol. The reaction is consistent with conjugate sulfur addition followed by intramolecular nitrogen attack and dehydration/cyclization to the seven-membered ring; the present data establish products but do not independently establish the detailed kinetic sequence.

### Antimicrobial assay

Antimicrobial screening used an agar-well diffusion format. Test compounds were prepared in 10% DMSO at 25, 50, 75 and 100 μg mL$^{-1}$. Inoculated nutrient-agar plates were rested for 30 min, 6-mm wells were prepared, and 30 μL of sample or standard was introduced. Bacterial plates were incubated at 37 °C for 24 h. Candida albicans was assessed on potato dextrose agar. Streptomycin served as the bacterial reference and ketoconazole as the fungal reference. Current CLSI documents describe standardized susceptibility methods and their quality-control requirements (Clinical and Laboratory Standards Institute [CLSI], 2024; Clinical and Laboratory Standards Institute [CLSI], 2026) accordingly, the present nonstandard exploratory well-diffusion results are not interpreted with clinical breakpoints.

### Fresh data analysis

The activity index (AI) was recalculated for every available cell as AI = Zcompound/Zreference, where Z is the inhibition-zone diameter at the same organism and concentration. Overall compound scores are arithmetic means across available AI values (15 or 16 cells, depending on missingness). High-dose scores are means across the four organisms at 100 μg mL$^{-1}$. For each matched substituent, series B minus series A differences were calculated only where both observations were available. Series-average dose curves use the mean across compounds; shaded bands show the observed compound minimum-to-maximum range and are not confidence intervals. Spearman correlations across the twelve compounds are exploratory. No hypothesis test comparing antimicrobial potency was considered confirmatory because independent biological replicate measurements and

within-condition variance were unavailable.

## Results

### Synthesis and physicochemical properties

All twelve target compounds were isolated in moderate yields (60–70%). Series A averaged 64.5% and series B averaged 66.3%. The narrow yield interval suggests that none of the six 8-substituents prevented cyclization under the common conditions. In contrast, melting points spanned 65–200 °C, with particularly high values for 5g and 5l. The physical-property distribution is summarized in Figure 1 and Table 1.

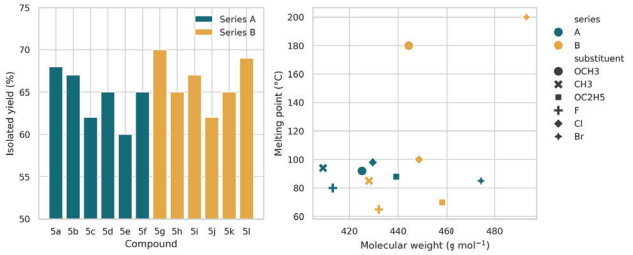


Figure 1. Synthetic and physical profile of the matched compound library. Bars show isolated yields; the scatterplot relates molecular weight to melting point. Series A contains the naphthyl scaffold and series B the 2,4-dichlorophenyl scaffold.

Table 1. Physicochemical characteristics and isolated yields of compounds 5a–5l.

| Cmpd | Series | 8-X | Formula/MW | mp (°C) | Rf | Yield (%) |
|---|---|---|---|---|---|---|
| 5a | A | $OCH_3$ | $C_{27}H_{23}NO_2S$ / 425.14 | 92 | .69 | 68 |
| 5b | A | $CH_3$ | $C_{27}H_{23}NOS$ / 409.15 | 94 | .65 | 67 |
| 5c | A | $OC_2H_5$ | $C_{28}H_{25}NO_2S$ / 439.16 | 88 | .68 | 62 |
| 5d | A | F | $C_{26}H_{20}FNOS$ / 413.12 | 80 | .66 | 65 |
| 5e | A | Cl | $C_{26}H_{20}ClNOS$ / 429.55 | 98 | .67 | 60 |
| 5f | A | Br | $C_{26}H_{20}BrNOS$ / 474.41 | 85 | .65 | 65 |
| 5g | B | $OCH_3$ | $C_{23}H_{19}Cl_2NO_2S$ / 444.30 | 180 | .63 | 70 |
| 5h | B | $CH_3$ | $C_{23}H_{19}Cl_2NOS$ / 428.00 | 85 | .47 | 65 |
| 5i | B | $OC_2H_5$ | $C_{24}H_{21}Cl_2NO_2S$ / 458.00 | 70 | .50 | 67 |
| 5j | B | F | $C_{22}H_{16}Cl_2FNOS$ / 432.00 | 65 | .78 | 62 |
| 5k | B | Cl | $C_{22}H_{16}Cl_3NOS$ / 448.50 | 100 | .85 | 65 |
| 5l | B | Br | $C_{22}H_{16}BrCl_2NOS$ / 493.00 | 200 | .86 | 69 |

### Spectroscopic and elemental characterization

The IR spectra supported ring formation and the expected substituent patterns. Series A displayed N–H stretching bands at 3502–3530 $cm^{-1}$, whereas series B showed lower-frequency N–H bands at 3136–3143 $cm^{-1}$. Aromatic and aliphatic C–H absorptions appeared in their expected regions, and series B consistently showed C–Cl-associated absorptions near 1025–1035 $cm^{-1}$. Methoxy/ethoxy-containing members also displayed C–O–C bands.

In the $^1$H NMR spectra, the diagnostic heterocyclic proton set was maintained across the library. The N–H signal occurred at δ 4.09–4.41, C2–H at δ 6.92–6.99, and C3–H at δ 7.50–8.15. The common 4-methoxy group appeared at δ 3.60–3.91. Additional singlets or ethyl triplet/quartet patterns confirmed the 8-methyl, 8-methoxy and 8-ethoxy substituents. Chlorinated representatives 5e and 5k showed molecular-ion isotope patterns consistent with chlorine, while bromo derivatives 5f and 5l showed the expected near-equal M/M+2 behavior. Elemental-analysis found values closely tracked calculated C, H, N and S percentages, providing orthogonal support for composition.

Table 2. Selected IR and $^1$H NMR diagnostic data.

| Cmpd | ν(N–H) | ν(ar C–H) | δ(N–H) | δ(C2–H) | δ(C3–H) | δ(4-$OCH_3$) |
|---|---|---|---|---|---|---|
| 5a | 3512 | 3092 | 4.35 | 6.92 | 8.15 | 3.60 |
| 5b | 3503 | 2982 | 4.12 | 6.98 | 7.81 | 3.78 |
| 5c | 3502 | 2963 | 4.20 | 6.99 | 7.81 | 3.78 |
| 5d | 3515 | 2996 | 4.41 | 6.97 | 7.84 | 3.78 |
| 5e | 3526 | 3098 | 4.30 | 6.98 | 7.88 | 3.69 |
| 5f | 3530 | 3025 | 4.18 | 6.96 | 8.03 | 3.68 |
| 5g | 3140 | 3002 | 4.13 | 6.98 | 7.81 | 3.80 |
| 5h | 3138 | 3007 | 4.09 | 6.99 | 7.84 | 3.85 |
| 5i | 3142 | 3001 | 4.12 | 6.92 | 7.82 | 3.91 |
| 5j | 3136 | 3010 | 4.10 | 6.96 | 7.85 | 3.88 |
| 5k | 3141 | 3005 | 4.12 | 6.94 | 7.80 | 3.90 |
| 5l | 3143 | 3009 | 4.11 | 6.92 | 7.50 | 3.80 |

Spectral assignments are reported as supportive characterization rather than complete constitutional proof. Future publication-grade characterization should include archived full spectra, $^{13}$C NMR, high-resolution mass measurements for every analogue and, where stereochemical or tautomeric questions matter, 2D NMR or crystallography.

### Global antimicrobial response

The compound library produced measurable inhibition against all four organisms. Most profiles increased with concentration, although small plate-based fluctuations were present. Figure 2 displays all recalculated activity indices. It also makes the major limitation visible: compound activity remained below the corresponding reference-drug zones in every measured cell. The best values therefore represent prioritization within this library, not equivalence to streptomycin or ketoconazole.

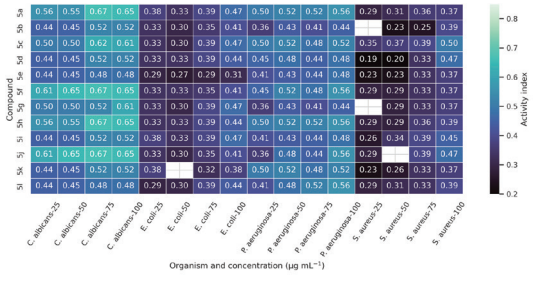


Figure 2. Recalculated activity-index matrix across compounds, organisms and concentrations. White cells denote source entries reported as NA and retained as missing. Activity index equals compound zone divided by

the concentration-matched reference-drug zone.

Series-level dose curves (Figure 3) show broadly similar mean responses for the two scaffolds. The compound ranges overlap at every organism–concentration combination. The strongest individual response was 19 mm for 5c against S. aureus at 100 µg mL$^{-1}$. This value corresponded to AI = 0.50 because the streptomycin reference zone was 38 mm. Against C. albicans, compounds 5a, 5f, 5h and 5j each reached 15 mm at 100 µg mL$^{-1}$ (AI = 0.65).

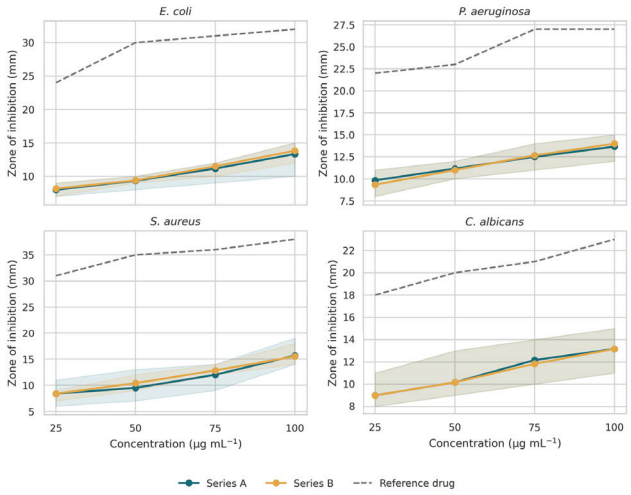


Figure 3. Series-average inhibition-zone response by concentration. Solid lines show compound means within each scaffold; shaded regions show the observed minimum–maximum range across compounds and are not inferential uncertainty intervals. Dashed gray lines show the reference drug.

## Compound ranking and high-dose activity

Compound 5j achieved the highest overall mean AI (0.465) across its 15 available cells. The next-ranked compounds were 5a (0.464) and 5c (0.460). Ranking by a mean of normalized values avoids giving disproportionate influence to organisms whose reference-drug zones are larger. Nevertheless, it is a screening score rather than a validated potency metric.

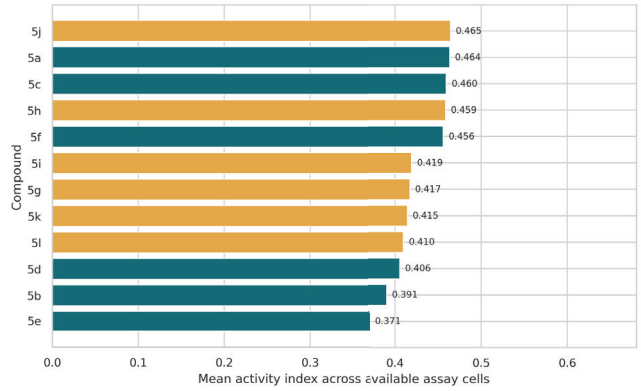


Figure 4. Descriptive compound ranking by mean activity index across all available organism–concentration cells. Teal bars denote series A and amber bars series B.

Table 3. Fresh descriptive ranking of antimicrobial performance.

| Cmpd | Series | 8-X | Mean zone | Mean AI | n | Zone @100 | AI @100 |
|---|---|---|---|---|---|---|---|
| 5j | B | F | 12.07 | 0.465 | 15 | 15.25 | 0.522 |
| 5a | A | OCH3 | 12.19 | 0.464 | 16 | 14.75 | 0.511 |
| 5c | A | OC2H5 | 12.31 | 0.460 | 16 | 15.50 | 0.524 |
| 5h | B | CH3 | 12.06 | 0.459 | 16 | 14.75 | 0.510 |
| 5f | A | Br | 11.88 | 0.456 | 16 | 14.25 | 0.496 |
| 5i | B | OC2H5 | 11.31 | 0.419 | 16 | 14.25 | 0.480 |
| 5g | B | OCH3 | 11.00 | 0.417 | 15 | 13.75 | 0.473 |
| 5k | B | Cl | 10.87 | 0.415 | 15 | 13.00 | 0.446 |
| 5l | B | Br | 11.00 | 0.410 | 16 | 13.75 | 0.467 |
| 5d | A | F | 10.81 | 0.406 | 16 | 14.25 | 0.479 |
| 5b | A | CH3 | 10.27 | 0.391 | 15 | 13.00 | 0.442 |
| 5e | A | Cl | 9.81 | 0.371 | 16 | 12.00 | 0.410 |

At the high dose, 5c remained the leading compound with a four-organism mean zone of 15.5 mm. Compounds 5a, 5h and 5f also maintained relatively broad high-dose effects. The organism-specific high-dose matrix (Figure 5) shows that rank order is not identical across taxa: 5c is distinguished by its S. aureus result, whereas 5f and 5h display balanced Gram-negative and antifungal profiles.

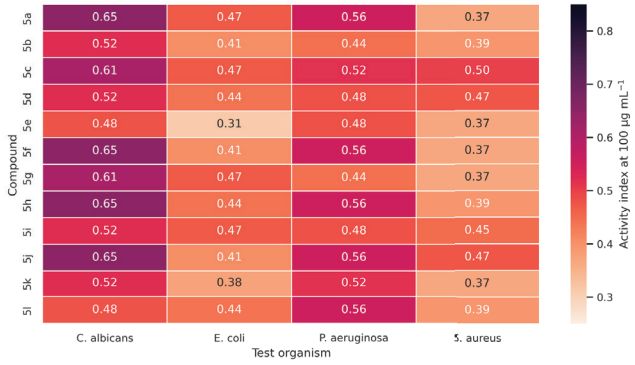


Figure 5. Organism-specific activity indices at 100 µg mL$^{-1}$. Values are normalized to streptomycin for bacteria and ketoconazole for C. albicans.

## Matched scaffold and substituent analysis

The paired design permits a focused question: for a fixed 8-substituent, did replacement of the naphthyl aryl domain by 2,4-dichlorophenyl consistently improve activity? The answer was no. Figure 6 and Table 4 show positive, negative and near-zero changes depending on substituent. The methyl pair favored 5h over 5b, whereas the ethoxy pair favored 5c over 5i. Methoxy, fluoro, chloro and bromo pairs showed smaller or context-dependent differences.

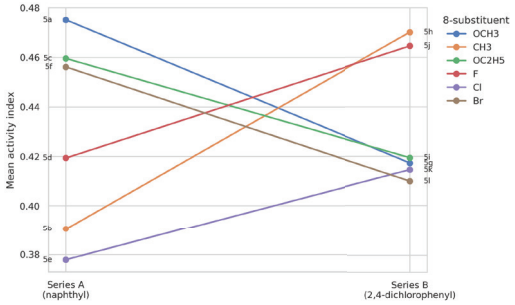


Figure 6. Matched comparison of the mean activity index for each 8-substituent in series A and B. Lines join analogues that differ in the

aryl scaffold. Labels identify compound codes.

Table 4. Matched scaffold comparison across mutually observed assay cells.

| 8-X | Series A | Series B | Mean AI A | Mean AI B | Δ(B–A) | Paired cells |
|---|---|---|---|---|---|---|
| OCH3 | 5a | 5g | 0.475 | 0.417 | -0.058 | 15 |
| CH3 | 5b | 5h | 0.391 | 0.470 | +0.080 | 15 |
| OC2H5 | 5c | 5i | 0.460 | 0.419 | -0.040 | 16 |
| F | 5d | 5j | 0.419 | 0.465 | +0.045 | 15 |
| Cl | 5e | 5k | 0.378 | 0.415 | +0.037 | 15 |
| Br | 5f | 5l | 0.456 | 0.410 | -0.046 | 16 |

These results argue against a simple 'more halogenation equals more activity' interpretation. Chlorine increases molecular weight and lipophilic character, but plate diffusion also depends on solubility, agar partitioning and diffusion rate. Thus, an analogue can have favorable target interactions yet yield a modest zone if transport through the assay matrix is limited (Balouiri et al., 2016; Bonev et al., 2008).

### Exploratory property–activity relationships

Across twelve compounds, molecular weight and overall mean AI showed a Spearman correlation of $\rho = 0.11$ (exploratory $p = 0.729$). The complete correlation matrix (Figure 7) should be interpreted cautiously because $n = 12$, multiple properties covary with scaffold identity, and the response values are not replicate means. The purpose is hypothesis generation. In particular, a strong correlation in this setting would not establish causation or a transferable quantitative structure–activity relationship.

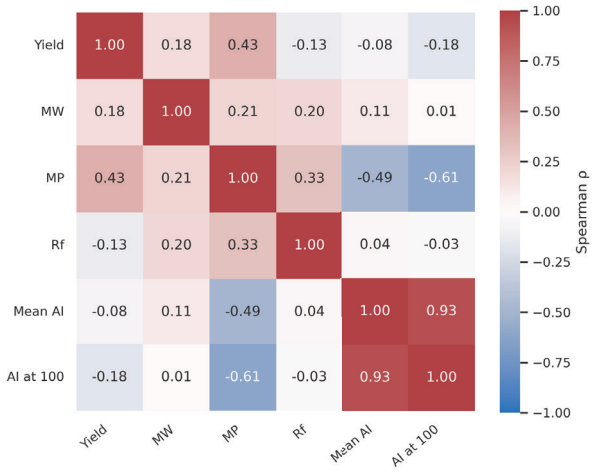


Figure 7. Exploratory Spearman rank-correlation matrix across the twelve compounds. AI denotes activity index. Correlations are descriptive and unadjusted for scaffold or multiple comparisons.

### Complete concentration–response dataset

Table 5 presents the complete inhibition-zone dataset as an integral part of the Results rather than as a detached annexure. Values are inhibition-zone diameters in millimetres at 25/50/75/100 µg $mL^{-1}$. A dash denotes a source entry reported as NA. Including the full matrix makes the compound rankings, normalization and missing-value decisions directly auditable.

#### E. coli

Table 5a. Complete inhibition-zone values for E. coli.

| Compound | 25 | 50 | 75 | 100 |
|---|---|---|---|---|
| 5a | 9 | 10 | 12 | 15 |
| 5b | 8 | 9 | 11 | 13 |
| 5c | 8 | 9 | 12 | 15 |
| 5d | 8 | 10 | 12 | 14 |
| 5e | 7 | 8 | 9 | 10 |
| 5f | 8 | 10 | 11 | 13 |
| 5g | 8 | 9 | 12 | 15 |
| 5h | 8 | 10 | 12 | 14 |
| 5i | 9 | 10 | 12 | 15 |
| 5j | 8 | 9 | 11 | 13 |
| 5k | 9 | — | 10 | 12 |
| 5l | 7 | 9 | 12 | 14 |
| Reference | 24 | 30 | 31 | 32 |

#### P. aeruginosa

Table 5b. Complete inhibition-zone values for P. aeruginosa.

| Compound | 25 | 50 | 75 | 100 |
|---|---|---|---|---|
| 5a | 11 | 12 | 14 | 15 |
| 5b | 8 | 10 | 11 | 12 |
| 5c | 11 | 12 | 13 | 14 |
| 5d | 10 | 11 | 12 | 13 |
| 5e | 9 | 10 | 12 | 13 |
| 5f | 10 | 12 | 13 | 15 |
| 5g | 8 | 10 | 11 | 12 |
| 5h | 11 | 12 | 14 | 15 |
| 5i | 9 | 10 | 12 | 13 |
| 5j | 8 | 11 | 12 | 15 |
| 5k | 11 | 12 | 13 | 14 |
| 5l | 9 | 11 | 14 | 15 |
| Reference | 22 | 23 | 27 | 27 |

#### S. aureus

Table 5c. Complete inhibition-zone values for S. aureus.

| Compound | 25 | 50 | 75 | 100 |
|---|---|---|---|---|
| 5a | 9 | 11 | 13 | 14 |
| 5b | — | 8 | 9 | 15 |
| 5c | 11 | 13 | 14 | 19 |
| 5d | 6 | 7 | 12 | 18 |
| 5e | 7 | 8 | 12 | 14 |
| 5f | 9 | 10 | 12 | 14 |
| 5g | — | 10 | 12 | 14 |
| 5h | 9 | 10 | 13 | 15 |
| 5i | 8 | 12 | 14 | 17 |
| 5j | 9 | — | 14 | 18 |
| 5k | 7 | 9 | 12 | 14 |
| 5l | 9 | 11 | 12 | 15 |
| Reference | 31 | 35 | 36 | 38 |

### C. albicans

Table 5d. Complete inhibition-zone values for C. albicans.

| Compound | 25 | 50 | 75 | 100 |
|---|---|---|---|---|
| 5a | 10 | 11 | 14 | 15 |
| 5b | 8 | 9 | 11 | 12 |
| 5c | 9 | 10 | 13 | 14 |
| 5d | 8 | 9 | 11 | 12 |
| 5e | 8 | 9 | 10 | 11 |
| 5f | 11 | 13 | 14 | 15 |
| 5g | 9 | 10 | 11 | 14 |
| 5h | 10 | 11 | 14 | 15 |
| 5i | 8 | 9 | 11 | 12 |
| 5j | 11 | 13 | 14 | 15 |
| 5k | 8 | 9 | 11 | 12 |
| 5l | 8 | 9 | 10 | 11 |
| Reference | 18 | 20 | 21 | 23 |

## Discussion

This reanalysis strengthens the thesis findings in three ways. First, it places every antimicrobial result on the same concentration-matched normalized scale. Second, it retains missing entries explicitly instead of converting them to inactivity. Third, it uses the matched-series structure to separate a broad scaffold comparison from substituent-specific behavior. Together, these steps produce a more defensible lead-prioritization narrative than isolated maximum-zone comparisons.

The synthetic results are consistent with the established utility of chalcone–o-aminothiophenol cyclocondensation for accessing 1,5-benzothiazepines (Chate et al., 2011; Mange et al., 2007; Suman et al., 2023). The 60–70% range is practically useful for small-library preparation and shows tolerance of both electron-donating and halogen substituents. Trifluoroacetic acid provides a simple homogeneous catalyst, although future process development should quantify reaction mass efficiency, solvent intensity and catalyst recovery in view of current interest in greener sulfur-heterocycle synthesis (Kosmalski et al., 2024; Ronse et al., 2023).

The antimicrobial pattern agrees qualitatively with prior reports that functionalized 1,5-benzothiazepines can display antibacterial and antifungal effects (Bhabal et al., 2022; Dhiaa et al., 2023; Haroun et al., 2022; Ogunnupebi et al., 2023; Wang et al., 2009, 2019, 2020). Direct numerical comparison across publications is inappropriate because strains, inoculum density, medium, well or disc geometry, solvent, dose and standards differ. Recent tetrazole-containing analogues were reported to show moderate antibacterial and antifungal activity but strong antitubercular effects (Suman et al., 2024). A 2026 study of related dihydrobenzothiazepines combined MIC testing with docking and ADMET analysis (Odame et al., 2026), while contemporary antimicrobial hybrid research increasingly pairs heterocycle synthesis with standardized MIC determination and target-focused modelling (Agarwal et al., 2025; Odame et al., 2023). These studies illustrate how appended pharmacophores and assay design can shift the apparent biological profile.

Compound 5c emerged as the most compelling high-dose lead in this dataset. It combined the largest four-organism mean zone at 100 μg $mL^{-1}$ with the best S. aureus zone and strong E. coli activity. Compound 5j had a slightly higher mean normalized score across available cells, but that score omits one condition and is therefore more sensitive to missingness; 5a had the highest mean AI among compounds with all sixteen observations. The 8-ethoxy substituent of 5c may support a favorable balance of hydrophobic contact and local polarity, but that mechanistic explanation remains speculative. The corresponding series-B ethoxy analogue 5i was weaker overall, demonstrating that substituent effects are conditional on the aryl domain.

Compounds 5f and 5h form a second priority tier. The bromo/naphthyl compound 5f maintained comparatively even activity across the panel and was among the strongest antifungal members. The methyl/dichlorophenyl compound 5h improved on its matched series-A analogue 5b and also showed balanced high-dose zones. These distinct profiles suggest that confirmatory testing should include multiple leads rather than only the top aggregate score. The lack of a uniform scaffold effect is chemically informative. Changing from a fused naphthyl group to a dichlorophenyl group alters shape, polarizability, conformational freedom and likely solubility simultaneously. Agar-zone diameter is particularly sensitive to diffusion. The matched differences therefore conflate intrinsic antimicrobial action with physical transport. Broth microdilution MIC values, kinetic growth curves and measured solubility would help distinguish these factors.

The current dataset cannot support statements of statistical significance between compounds. Each condition is represented by one reported zone and the source does not provide independent plate replicates, standard deviations or raw images. Treating the sixteen dose–organism cells as biological replicates would create pseudoreplication because they differ systematically in organism and concentration. We therefore restricted the analysis to transparent descriptive summaries. This limitation should be stated plainly during submission.

Future microbiology should follow recognized quality-control guidance (Clinical and Laboratory Standards Institute [CLSI], 2024; Clinical and Laboratory Standards Institute [CLSI], 2026). At minimum, confirmatory work should use authenticated strains, standardized inocula, solvent and blank controls, three independent experiments, randomized plate layouts and blinded zone reading. MIC and minimum bactericidal/fungicidal concentrations should be determined by broth dilution. Cytotoxicity in a mammalian cell line would permit selectivity-index estimation, and time-kill or membrane-integrity assays could begin to address mechanism.

Chemically, complete $^{13}C$ NMR and HRMS for all compounds would upgrade identity assurance. Purity should be quantified by HPLC or qNMR before biological retesting. The unusually high melting points of 5g and 5l could reflect crystal packing or polymorphism and merit DSC or powder X-ray analysis. These steps are important because biological rank differences are modest and could be distorted by purity or dissolution differences.

Taken together, the findings position this library as a useful starting point rather than a finished antimicrobial series. The strongest value lies in its matched substitution design: it demonstrates which structural changes should be carried forward into a more rigorous second-generation experiment.

## Limitations

- The source provides single reported inhibition-zone values and no replicate-level variance.
- Agar-well diffusion is influenced by solubility and diffusion

and does not yield MIC values.
- Four source cells were marked NA; the reason for missingness was not documented.
- Strain identifiers, inoculum standardization details and compound purity percentages were not reported in the analyzed chapter.
- Correlations use only twelve compounds and are vulnerable to scaffold confounding and multiple testing.
- No mammalian cytotoxicity or selectivity data were available.

These limitations affect different parts of the interpretation. Missing replication prevents estimation of experimental precision and formal between-compound testing. Missing strain and inoculum details limit external reproducibility. The diffusion format further prevents a clean separation of intrinsic growth inhibition from compound transport through agar. None of these issues invalidates the recorded screening pattern, but together they restrict the appropriate claim to comparative lead prioritization.

### Recommended confirmatory study

A compact second-stage experiment can resolve the major uncertainties while conserving material. Compounds 5c, 5a, 5f and 5h should be advanced, with 5e retained as a lower-ranked internal comparator. Each should be purity-qualified before testing. The same four organisms should be used initially to preserve continuity, but authenticated strain identifiers and inoculum density must be recorded. Broth microdilution should be the primary potency assay, with well diffusion retained only as a historical bridge to the thesis dataset.

Table 6. Minimum evidence package proposed for lead confirmation.

| Question | Recommended measurement | Design safeguard | Decision output |
|---|---|---|---|
| Identity/purity | $^{13}$C NMR, HRMS and HPLC or qNMR purity | Predefine ≥95% purity for biological comparison | Qualified test articles |
| Reproducibility | Three independent experiments on separate days | Randomized plate map; blinded reading | Mean, SD and confidence intervals |
| Potency | Twofold broth-microdilution MIC series | CLSI-aligned inoculum and QC strains | MIC distribution and rank |
| Killing effect | MBC/MFC and time-kill for top two leads | Vehicle and reference-drug controls | Static versus cidal behavior |
| Selectivity | Mammalian-cell viability over matched range | Same solvent exposure as microbial assay | Cytotoxicity and selectivity index |
| Mechanism | Membrane integrity or leakage screen | Orthogonal positive/negative controls | Testable mode-of-action hypothesis |

## Conclusions

Twelve 8-substituted 2,5-dihydro-1,5-benzothiazepines were synthesized in 60–70% yield and characterized by complementary spectroscopic and elemental methods. Fresh analysis of the available antimicrobial matrix identified 5c as the high-dose leader, 5a as the strongest complete-profile normalized performer, and 5f and 5h as additional balanced candidates; 5j's highest available-cell mean should be treated cautiously because one condition was missing. Responses generally increased with concentration, but remained below the reference drugs. Matched comparisons showed that the naphthyl-to-dichlorophenyl scaffold exchange did not confer a universal advantage; its effect depended on the 8-substituent and test organism. These conclusions are appropriately descriptive because replicate-level measurements were unavailable. Confirmatory MIC testing, biological replication, quantitative purity assessment and cytotoxicity evaluation are the next essential steps.

## References


World Health Organization. (2025). Global antibiotic resistance surveillance report 2025. *World Health Organization*.

Clinical and Laboratory Standards Institute. (2024). M02: Performance standards for antimicrobial disk susceptibility tests (14th ed.). *Clinical and Laboratory Standards Institute*.

Clinical and Laboratory Standards Institute. (2026). M27M44S: Performance standards for antifungal susceptibility testing of yeasts. *Clinical and Laboratory Standards Institute*.

Ogunnupebi, T. A., et al. (2023). Chemistry and pharmacological diversity of benzothiazepine. *Pharmaceuticals*, 16, 314. https://doi.org/10.3390/ph16020314

Bariwal, J. B., Upadhyay, K. D., Manvar, A. T., Trivedi, J. C., Singh, J. S., Jain, K. S., & Shah, A. K. (2008). 1,5-Benzothiazepine, a versatile pharmacophore: A review. *European Journal of Medicinal Chemistry*, 43, 2279–2290. https://doi.org/10.1016/j.ejmech.2008.05.035

Saha, D., Jain, G., & Sharma, A. (2015). Benzothiazepines: Chemistry of a privileged scaffold. *RSC Advances*, 5, 70619–70639. https://doi.org/10.1039/C5RA12422K

Dhiaa, S., Mohammed, S., Bahir, H., et al. (2023). Recent advances in bioactive 1,5-benzothiazepine-based compounds: Highlights from 2012 to 2022. *Chemistry Review Letters*, 6, 390–402.

Haroun, M., Chobe, S. S., Alavala, R. R., et al. (2022). 1,5-Benzothiazepine derivatives: Green synthesis, in silico and in vitro evaluation as anticancer agents. *Molecules*, 27, 3757. https://doi.org/10.3390/molecules27123757

Suman, A. K., Anu, A., & Singh, B. (2024). Synthesis and in vitro evaluation of tetrazole containing 1,5-benzothiazepines as new anticancer, antitubercular, antibacterial, and antifungal agents. *European Journal of Chemistry*, 15, 245–253. https://doi.org/10.5155/eurjchem.15.3.245-253.2569

Suman, A. K., Dushad, A., & Singh, B. (2023). 1,5-Benzothiazepines: Recent developments in the synthetic strategies. *Tetrahedron*, 142, 133513. https://doi.org/10.1016/j.tet.2023.133513

Ronse, U., Magdalenić, K., Van Camp, J., & D'hooghe, M. (2023). Synthesis of the 1,5-benzothiazepane scaffold—Established methods and new developments. *ChemistryOpen*, 12, e202200262. https://doi.org/10.1002/open.202200262

Kosmalski, T., et al. (2024). The application of green solvents in the synthesis of S-heterocyclic compounds. International *Journal of Molecular Sciences*, 25, 9474. https://doi.org/10.3390/ijms25179474

Devi, V., Singh, G., & Monga, V. (2020). Recent advances in the synthetic chemistry of 1,5-benzothiazepines: A minireview. *Journal of Heterocyclic Chemistry*, 57, 3255–3270. https://doi.org/10.1002/jhet.4062

Pathania, S., Narang, R. K., & Rawal, R. K. (2019). Role of sulphur-heterocycles in medicinal chemistry: An update. *European Journal of Medicinal Chemistry*, 180, 486–508. https://doi.org/10.1016/j.ejmech.2019.07.043

Chate, A. V., Joshi, R. S., Mandhane, P. G., & Gill, C. H. (2011). An improved procedure for the synthesis of 1,5-benzothiazepines using ceric ammonium nitrate. *Journal of the Korean Chemical Society*, 55, 776–780. https://doi.org/10.5012/jkcs.2011.55.5.776

Mange, S., Singh, H. P., Gupta, S. D., & Moorthy, N. S. H. N. (2007). Synthesis and characterization of some chalcone derivatives. *Trends in Applied Sciences Research*, 2, 52–56. https://doi.org/10.3923/tasr.2007.52.56

Balouiri, M., Sadiki, M., & Ibnsouda, S. K. (2016). Methods for in vitro evaluating antimicrobial activity: A review. *Journal of Pharmaceutical Analysis*, 6, 71–79. https://doi.org/10.1016/j.jpha.2015.11.005

Bonev, B., Hooper, J., & Parisot, J. (2008). Principles of assessing bacterial susceptibility to antibiotics using the agar diffusion method. J*ournal of Antimicrobial Chemotherapy*, 61, 1295–1301. https://doi.org/10.1093/jac/dkn090

Wang, L., Zhang, P., Zhang, X., Zhang, Y., Li, Y., & Wang, Y. (2009). Synthesis and biological evaluation of a novel series of 1,5-benzothiazepine derivatives as potential antimicrobial agents. *European Journal of Medicinal Chemistry*, 44, 2815–2821. https://doi.org/10.1016/j.ejmech.2008.12.021

Wang, R., Wang, Y., Bian, Y., & Zhang, P. (2020). Synthesis and antifungal activity of 1,5-benzothiazepines containing 1,2,3-triazole. *Chinese Journal of Organic Chemistry*, 40, 398–407. https://doi.org/10.6023/cjoc201907056

Wang, Y., Kong, L., Wang, R., Tian, K., & Zhang, P. (2019). Synthesis and antimicrobial activity of C(3)-1,2,4-triazolyl-1,5-benzothiazepines. C*hinese Journal of Organic Chemistry*, 39, 2663–2670. https://doi.org/10.6023/cjoc201901041

Bhabal, S. R., Shaikh, S., Yellapurkar, I., Pavale, G., & Ramana, M. M. V. (2022). Synthesis of novel fluorinated 1,5-benzothiazepine derivatives and their biological evaluation as anticancer and antibacterial agents. *Journal of the Serbian Chemical Society*. https://doi.org/10.2298/JSC210428041B

Shaik, A. B., Prasad, Y. R., Nissankararao, S., & Shahanaaz, S. (2020). Synthesis, biological and computational evaluation of novel 2,3-dihydro-1,5-benzothiazepines as anticancer and anti-EGFR agents. *Anti-Cancer Agents in Medicinal Chemistry*, 20, 1115–1128. https://doi.org/10.2174/1871520620666200130091142

Kaur, R., Singh, R., & Singh, K. (2016). 1,5-Benzothiazepine: Bioactivity and targets. *Chemical and Biological Letters*, 3, 18–31.

Feng, M., Tang, B., Liang, S. H., & Jiang, X. (2016). Sulfur containing scaffolds in drugs: Synthesis and application in medicinal chemistry. *Current Topics in Medicinal Chemistry*, 16, 1200–1216. https://doi.org/10.2174/1568026615666150915111741

Gharge, S., & Alegaon, S. G. (2024). Recent studies of nitrogen and sulfur containing heterocyclic analogues as novel antidiabetic agents: A review. *Chemistry & Biodiversity*, 21, e202301738. https://doi.org/10.1002/cbdv.202301738

Odame, F., Ayivor-Djanie, R., Madanhire, T., et al. (2026). Synthesis, characterization, antimicrobial activity, docking, and in silico ADMET analysis of some new 2,3-dihydrobenzo[b][1,4]thiazepine derivatives. *BioMed Research International*, 2026, 5076755. https://doi.org/10.1155/bmri/5076755

Agarwal, A., Singh, V., Maurya, A., et al. (2025). Design, synthesis, and antimicrobial evaluation of new triazole-tethered tetrazole hybrids via DNA gyrase inhibition. *Scientific Reports*, 15, 34695. https://doi.org/10.1038/s41598-025-15919-4

Qadir, T., Amin, A., Sharma, P. K., Jeelani, I., & Abe, H. (2022). A review on medicinally important heterocyclic compounds. *The Open Medicinal Chemistry Journal*, 16, e187410452202280. https://doi.org/10.2174/187410452202280

Chaudhri, V. K. (2022). 1,5-Benzothiazepine: As potential biologically active agent. *Der Pharma Chemica, 14*(10), 19–33. https://doi.org/10.4172/0975-413X.14.10.19-33

Odame, F., Madanhire, T., Tettey, C., et al. (2023). Anticancer and antimicrobial activity of some new 2,3-dihydro-1,5-benzodiazepine derivatives. *Heteroatom Chemistry*, 2023, 3390122. https://doi.org/10.1155/2023/3390122